help to code the perception of "flavor" [e.g., responding to several tastes simultaneously (24, 26, 42)]. In addition, the insular cortex responds to more than just taste, and it is often thought of as a site for multisensory integration (15, 42, 43). Thus, these areas may participate in the integration of taste with the other senses.

The discovery of a gustotopic map in the mammalian cortex, together with the advent of sophisticated genetic and optical tools (44), should now make it possible to experimentally manipulate the taste cortex with exquisite finesse. In future studies, it will also be important to elucidate how taste intensity is encoded in the insular cortex, and to determine whether taste qualities with similar valence project to common targets. Likewise, tracing the connectivity of each of the basic taste qualities to higher brain stations will help decipher how these integrate with other modalities and combine with internal and emotional states to ultimately choreograph taste behaviors (45).

References and Notes

1. X. Li et al., Proc. Natl. Acad. Sci. U.S.A. **99**, 4692 (2002).
2. G. Nelson et al., Nature **416**, 199 (2002).
3. G. Q. Zhao et al., Cell **115**, 255 (2003).
4. G. Nelson et al., Cell **106**, 381 (2001).
5. E. Adler et al., Cell **100**, 693 (2000).
6. J. Chandrashekar et al., Cell **100**, 703 (2000).
7. H. Matsunami, J.-P. Montmayeur, L. B. Buck, Nature **404**, 601 (2000).
8. K. L. Mueller et al., Nature **434**, 225 (2005).
9. J. Chandrashekar, M. A. Hoon, N. J. Ryba, C. S. Zuker, Nature **444**, 288 (2006).
10. A. L. Huang et al., Nature **442**, 934 (2006).
11. Y. Ishimaru et al., Proc. Natl. Acad. Sci. U.S.A. **103**, 12569 (2006).
12. J. Chandrashekar et al., Nature **464**, 297 (2010).
13. Y. Zhang et al., Cell **112**, 293 (2003).
14. D. A. Yarmolinsky, C. S. Zuker, N. J. Ryba, Cell **139**, 234 (2009).
15. S. A. Simon, I. E. de Araujo, R. Gutierrez, M. A. Nicolelis, Nat. Rev. Neurosci. **7**, 890 (2006).
16. D. D. Stettler, R. Axel, Neuron **63**, 854 (2009).
17. M. M. Merzenich, P. L. Knight, G. L. Roth, J. Neurophysiol. **38**, 231 (1975).
18. R. J. Tusa, L. A. Palmer, A. C. Rosenquist, J. Comp. Neurol. **177**, 213 (1978).
19. T. A. Woolsey, H. Van der Loos, Brain Res. **17**, 205 (1970).
20. R. Accolla, B. Bathellier, C. C. Petersen, A. Carleton, J. Neurosci. **27**, 1396 (2007).
21. H. Yoshimura, T. Sugai, M. Fukuda, N. Segami, N. Onoda, Neuroreport **15**, 17 (2004).
22. M. Sugita, Y. Shiba, Science **309**, 781 (2005).
23. E. S. Soares et al., Physiol. Behav. **92**, 629 (2007).
24. J. R. Stapleton, M. L. Lavine, R. L. Wolpert, M. A. Nicolelis, S. A. Simon, J. Neurosci. **26**, 4126 (2006).
25. T. Yamamoto, Prog. Neurobiol. **23**, 273 (1984).
26. A. Carleton, R. Accolla, S. A. Simon, Trends Neurosci. **33**, 326 (2010).
27. D. B. Katz et al., J. Neurosci. **28**, 11802 (2008).
28. J. N. Kerr et al., J. Neurosci. **27**, 13316 (2007).
29. K. Ohki, S. Chung, Y. H. Ch'ng, P. Kara, R. C. Reid, Nature **433**, 597 (2005).
30. C. Stosiek, O. Garaschuk, K. Holthoff, A. Konnerth, Proc. Natl. Acad. Sci. U.S.A. **100**, 7319 (2003).
31. C. N. Cearley et al., Mol. Ther. **16**, 1710 (2008).
32. See supporting material on Science Online.
33. T. Komiyama et al., Nature **464**, 1182 (2010).
34. S. V. Wu, M. C. Chen, E. Rozengurt, Physiol. Genomics **22**, 139 (2005).
35. K. Iwasaki, T. Kasahara, M. Sato, Physiol. Behav. **34**, 531 (1985).
36. We used the monopotassium form of glutamate to prevent confounding activity from a potential sodium taste hot spot (3).
37. S. C. Kinnamon, R. F. Margolskee, Curr. Opin. Neurobiol. **6**, 506 (1996).
38. T. Arai, T. Ohkuri, K. Yasumatsu, T. Kaga, Y. Ninomiya, Neuroscience **165**, 1476 (2010).
39. A. Caicedo, K. N. Kim, S. D. Roper, J. Physiol. **544**, 501 (2002).
40. T. A. Gilbertson, J. D. Boughter Jr., H. Zhang, D. V. Smith, J. Neurosci. **21**, 4931 (2001).
41. T. Sato, L. M. Beidler, Chem. Senses **22**, 287 (1997).
42. D. B. Katz, S. A. Simon, M. A. Nicolelis, J. Neurosci. **21**, 4478 (2001).
43. M. Kadohisa, E. T. Rolls, J. V. Verhagen, Chem. Senses **30**, 401 (2005).
44. L. Fenno, O. Yizhar, K. Deisseroth, Annu. Rev. Neurosci. **34**, 389 (2011).
45. A. Fontanini, D. B. Katz, Ann. N.Y. Acad. Sci. **1170**, 403 (2009).

REPORTS

Vacuum-Induced Transparency

Haruka Tanji-Suzuki,[1,2]* Wenlan Chen,[2] Renate Landig,[2] Jonathan Simon,[1] Vladan Vuletić[2]

Photons are excellent information carriers but normally pass through each other without consequence. Engineered interactions between photons would enable applications as varied as quantum information processing and simulation of condensed matter systems. Using an ensemble of cold atoms strongly coupled to an optical cavity, we found that the transmission of light through a medium may be controlled with few photons and even by the electromagnetic vacuum field. The vacuum induces a group delay of 25 nanoseconds on the input optical pulse, corresponding to a light velocity of 1600 meters per second, and a transparency of 40% that increases to 80% when the cavity is filled with 10 photons. This strongly nonlinear effect provides prospects for advanced quantum devices such as photon number–state filters.

The experimental realization of strong coherent interactions between individual photons will enable a variety of applications such as quantum computing (1–3) and studies of strongly correlated many-body quantum systems (4). Two main approaches to generating photon-photon interactions are strong coupling of single emitters to optical cavities (2, 3, 5–9) and electromagnetically induced transparency (EIT) in ensembles of atoms (10–12). Single emitters strongly coupled to cavities can provide substantial optical nonlinearity at the expense of typically large input-output coupling losses and the technical challenges of trapping and manipulating single particles. EIT in atomic ensembles provides an impressive degree of coherent control in simple, elegant experiments (12–15), but the nonlinearities achieved so far are relatively weak, requiring (for example) ~500 photons for all-optical switching (16). We demonstrate that by using an optical cavity to enhance the EIT control field, the resonant transmission of light through an atomic ensemble can be substantially altered by a few photons and even by the cavity vacuum (17, 18). Because the effect is nonlinear in both control and probe fields at the single-photon level, it should enable advanced quantum optical devices such as photon number–state filters (19) and nondestructive photon number–resolving detectors (20, 21). We call the limiting case with no photons initially in the cavity "vacuum-induced transparency" (VIT) (17) to distinguish it from recent cavity EIT demonstrations using a single atom with cavity-enhanced absorption and a classical control field containing many photons (22, 23). In contrast, VIT may be realized with only one photon in the entire system.

We experimentally realize Field's original proposal (17) to replace the EIT control field by the vacuum field inside a strongly coupled cavity (Fig. 1). In an atomic Λ system $|f\rangle \leftrightarrow |e\rangle \leftrightarrow |g\rangle$ with two stable states $|f\rangle$, $|g\rangle$, the probe beam addresses the $|f\rangle \rightarrow |e\rangle$ transition, whereas the cavity mode is tuned near the $|g\rangle \rightarrow |e\rangle$ transition. A cold atomic ensemble is prepared in the state $|f\rangle$ by optical pumping. VIT for the probe beam can be thought of as arising from a vacuum-induced Raman process where the incoming probe photon is absorbed, quickly emitted into the cavity, then reabsorbed by the ensemble and reemitted

[1]Department of Physics, Harvard University, Cambridge, MA 02138, USA. [2]Department of Physics, MIT-Harvard Center for Ultracold Atoms, and Research Laboratory of Electronics, Massachusetts Institute of Technology, Cambridge, MA 02139, USA.

*To whom correspondence should be addressed. E-mail: haruka.tanji@post.harvard.edu

collectively back into the probe mode. Thus, the incoming probe photon creates its own transparency by destructive interference in the excited state $|e\rangle$ arising from the two transitions $|f\rangle \to |e\rangle$ and $|g\rangle \to |e\rangle$. In contrast to standard EIT, here the effective control field on the $|g\rangle \to |e\rangle$ transition depends sensitively on the photon number in the probe field. When there are several photons in the probe field, those photons are coupled to the cavity mode, constituting an effective probe power–dependent control field for the VIT process. Because the EIT group delay depends on the control coupling strength (12), different probe Fock states experience different group delay and therefore an incoming coherent-state probe pulse may be resolved into a train of photon number components (19).

VIT requires strong coupling between a single atom and a cavity—that is, a single-atom cooperativity parameter $\eta_0 = 4g^2/(\kappa\Gamma)$ exceeding unity [where $2g$, κ, and Γ are the single-photon Rabi frequency, cavity line width, and atomic line width (full width at half maximum), respectively]. For unity oscillator strength, the cooperativity parameter is a geometric quantity associated with the cavity characteristics alone and can be written in terms of the finesse $\mathcal{F}$, waist w, and wave number k of the cavity mode as $\eta_0 = 24\mathcal{F}/(\pi k^2 w^2)$ (24). Our parameters $\lambda = 2\pi/k = 852$ nm, $w = 35$ μm, and $\mathcal{F} = 6.3 \, (\pm 0.5) \times 10^4$ yield a maximum cooperativity for a single ^{133}Cs atom at an antinode of $\eta_0 = 7.2 \pm 0.5$. The actual cooperativity η available in the experiment is smaller because of oscillator strength $f_{eg} < 1$ for the $|g\rangle \leftrightarrow |e\rangle$ transition in question, and also because of spatial averaging of the coupling along the standing-wave cavity mode.

For probe light illuminating the ensemble from the side (Fig. 1), the amplitude transfer function $t = \exp(ikL\chi/2)$ can be expressed in terms of the susceptibility χ that in the limit of weak coupling on the probe transition (single probe photon) is given by

$$\chi = -\frac{\mathcal{N}}{kL}\frac{\tilde{\Delta} - (\eta - \tilde{\Delta}\tilde{\delta})\tilde{\delta} - i(\eta + 1 + \tilde{\delta}^2)}{(\eta + 1 - \tilde{\Delta}\tilde{\delta})^2 + (\tilde{\Delta} + \tilde{\delta})^2} \quad (1)$$

(12, 17, 18), where $\mathcal{N}$ is the resonant optical depth of the ensemble with length L along the probe beam, and $\tilde{\Delta} = 2\Delta/\Gamma = 2(\omega_p - \omega_{ef})/\Gamma$ and $\tilde{\delta} = 2(\Delta - \delta)/\kappa = 2(\omega_p - \omega_c - \omega_{gf})/\kappa$ are the normalized probe-atom detuning and the "two-photon" detuning, respectively (Fig. 1B), where ω_p, ω_c, and ω_{ji} are the frequencies of the probe, cavity mode, and atomic transition $|i\rangle \to |j\rangle$, respectively. Equation 1 can be obtained from the standard EIT expression (12) with states $|f; n_p = 1; n_c = 0\rangle$, $|e; 0; 0\rangle$, $|g; 0; 1\rangle$, where n_p and n_c are the probe and cavity photon numbers, respectively, with the cavity line width κ assigned to the state $|g; 0; 1\rangle$ (17). When both the probe field and the cavity mode are resonant with their respective atomic transitions, $\Delta = \delta = 0$, the transmission probability is given by $|t|^2 = \exp[-\mathcal{N}/(\eta + 1)]$—that is, the resonant optical depth $\mathcal{N}$ is reduced by a factor $\eta + 1$ by the cavity vacuum field.

The observation of VIT requires substantial atomic absorption in a transverse direction for an optical cavity that operates in the strong coupling limit $\eta > 1$ for a single atom (5, 7, 8). This parameter regime has recently been achieved with evaporatively cooled atoms in cavities with small mode volume (25–27). Here we use a relatively long (1.4 cm) cavity that allows us to operate a magneto-optical trap for ^{133}Cs inside the cavity, and directly load up to 10^5 atoms into a far-off resonance optical lattice trap operated at 937 nm inside the cavity. The three-level system is chosen as $|f\rangle \equiv |6S_{1/2}, F = 3, m_F = 3\rangle$, $|e\rangle \equiv |6P_{3/2}, 4, 4\rangle$, $|g\rangle \equiv |6S_{1/2}, 4, 4\rangle$ to provide a good combination of oscillator strengths in both arms ($f_{ef} = 0.42$, $f_{eg} = 0.47$). The quantization axis is defined by a 1.6-G magnetic field along the propagation direction (x) of the probe beam

Fig. 1. (**A** and **B**) Setup (A) and atomic level scheme (B) for observing vacuum-induced transparency. An ensemble of laser-cooled ^{133}Cs atoms is trapped inside an optical cavity operating in the single-atom strong-coupling regime (cooperativity parameter $\eta > 1$). The atoms are prepared in state $|f\rangle$ by optical pumping. The absorption of a probe laser on the transition $|f\rangle \leftrightarrow |e\rangle$ is substantially altered when a cavity mode on the transition $|g\rangle \leftrightarrow |e\rangle$ is tuned near two-photon resonance. Although the cavity mode subtends only a very small (~10^{-4} sr) solid angle along a direction transverse to the probe beam, its vacuum field can substantially reduce the probe absorption by quantum interference. Photon counters D1 and D2 are used to measure the probe transmission and the scattering into the cavity, respectively.
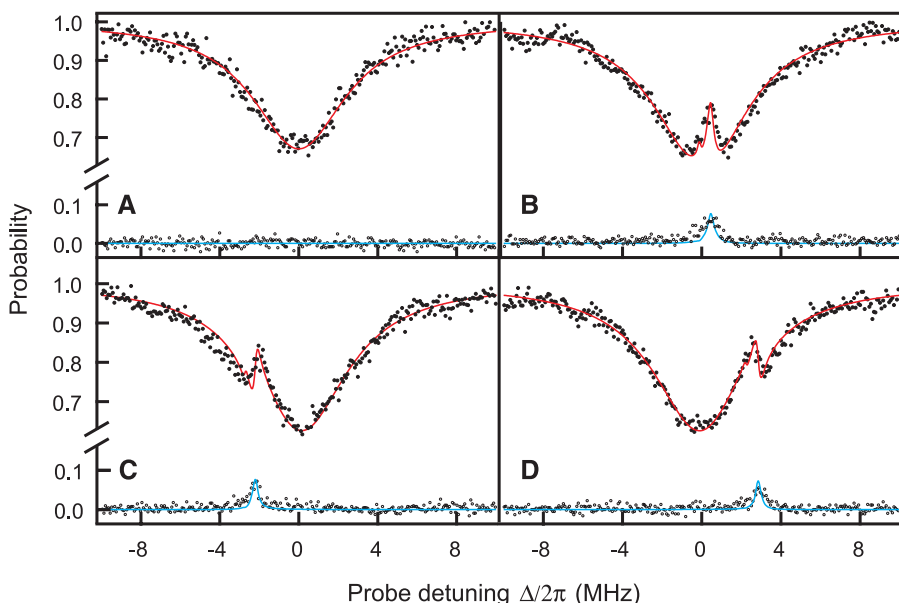
Fig. 2. (**A** to **D**) Atomic absorption spectrum (A) and VIT spectra (B to D) for different cavity-atom detunings: (B) $\delta/(2\pi) = 0.5$ MHz, (C) $\delta/(2\pi) = -2.2$ MHz, (D) $\delta/(2\pi) = 2.8$ MHz. The transmission probability (upper curves) and the probability of emission into the cavity (lower curves) are measured simultaneously versus probe-atom detuning Δ by photon-counting detectors D1 and D2. Near the two-photon resonance $\Delta \approx \delta$ the absorption is suppressed by VIT, and a fraction of the incoming photons is directed out of the cavity. Data for both processes for all values of δ are simultaneously described by the VIT model explained in the text (solid lines).

(Fig. 1). The σ^+-polarized probe beam is tightly focused by an aspheric lens to a waist $w_p = 2.3$ µm at the cavity mode. We achieve an optical depth up to $\mathcal{N} = 0.4$ by optically pumping all atoms into the $F = 3$ hyperfine manifold, and more than 90% into state $|g\rangle$. The thickness of the cloud along the probe beam is $L = 20$ µm at a typical temperature of 100 µK, with an estimated peak atomic density of 1.1×10^{11} cm^{-3}. Typically, ~20 atoms are contained in the volume defined by the probe beam.

With the cavity mode tuned far off resonance from the $|g\rangle \leftrightarrow |e\rangle$ transition, the probe frequency is scanned across the $|f\rangle \rightarrow |e\rangle$ resonance, revealing a Lorentzian absorption profile with a line width of 5.46 ± 0.07 MHz (Fig. 2A), where the slight broadening over the natural line width $\Gamma/(2\pi) = 5.2$ MHz is due to the laser line width. When the cavity mode is tuned close to the $|g\rangle \leftrightarrow |e\rangle$ transition, a transparency window opens up around the $|f\rangle \leftrightarrow |g\rangle$ two-photon transition frequency (Fig. 2, B to D). To prevent the accumulation of atoms incoherently pumped by the trapping light into the $F = 4$ hyperfine state whose absorption would spoil the cavity finesse, the probe field is turned on and off every 4 µs during the 2.5-ms frequency scan, and a depumping beam emptying the $F = 4$ hyperfine state is turned on during the probe dark times. The 4-µs duration of the probe pulses is chosen so that the modulation-induced frequency broadening is smaller than the cavity line width $\kappa/(2\pi) = 173 \pm 13$ kHz. To probe the steady-state response of the system as described by Eq. 1, we restrict the analysis to times $t \geq 0.5$ µs where transients associated with the width of the transparency window $(1 + \eta)\kappa$ have decayed. At a probe power of 220 fW and an optical depth of $\mathcal{N} = 0.4$, we only analyze data corresponding to times $t < 2.6$ µs such that the total number of absorbed photons is $0.8 < 1$.

The VIT spectra for various atom-cavity detunings, as well as the accompanying photon leakage from the cavity mode (Fig. 2, B to D), can be simultaneously fit to the VIT model, Eq. 1. Although the vacuum Rabi splitting is not observable in our parameter regime ($\eta > 1$ but $2g < \Gamma$), the transparency in a narrow window is clearly visible because of quantum interference. The observed resonance is slightly broader than predicted by the model because of a small, independently observed line broadening of 200 kHz resulting from atom-induced shifts of the cavity mode frequency that fluctuate with the number of loaded atoms. The spectra also reveal a small contribution from the VIT transition $|f\rangle \leftrightarrow |e\rangle \leftrightarrow |6S_{1/2}, 4, 3\rangle$, weaker by a factor of 4, that is two-photon Zeeman-shifted by 0.6 MHz.

As in standard EIT, the index of refraction $n = \sqrt{1 + \mathrm{Re}(\chi)}$ is unity on resonance $\Delta = \delta = 0$ and varies sharply with probe frequency ω_p for fixed cavity detuning $\delta = 0$, giving rise to a reduced probe group velocity $v_g = c/[n + (\omega_p dn/d\omega_p)] \ll c$ (11, 12, 15). Pulses that are sufficiently narrow spectrally to fit into the transparency window

should therefore, according to Eq. 1, experience a maximum group delay (12) of $\tau_{max} = (\mathcal{N}/\kappa)[\eta/(\eta + 1)^2]$. During this delay time, the incoming probe photon is in part stored as a stationary photon inside the optical cavity for up to a time κ^{-1}, while a spin excitation with one atom in state $|g\rangle$ is simultaneously created in the ensemble. The delay decreases with increasing η, because a stronger control field reduces the population in state $|g\rangle$, and a smaller fraction of the photon is stored in the cavity accordingly. Figure 3 shows a Gaussian pulse of $T_P = 1.73$ µs duration that is delayed by the vacuum by $\tau = 25 \pm 2$ ns, close to the value of 35 ns calculated from Eq. 1 for the measured optical depth $\mathcal{N} = 0.5$ (achieved in a double-pass geometry). The small discrepancy is explained by small (~200 kHz) atom-induced fluctuations of the cavity resonance frequency as described above. Although the absolute delay τ, corresponding to a group velocity of $v = 1600$ m/s, is small in the present system because of the relatively small optical depth $\mathcal{N}$, the observation nonetheless establishes experimentally that a vacuum input control field can delay a probe pulse. Larger delays can be achieved by increasing $\mathcal{N}$, either by enhancing the atomic density via further optical cooling (28) or by means of a multipass geometry for the probe beam.

Unlike standard EIT, the VIT process is intrinsically nonlinear at the single-photon level: In EIT the classical control field with very large photon number $\langle n_c \rangle \gg 1$ alone determines the transparency window and group velocity of the probe light (12, 15); there is no dependence on the weak probe field with photon number $\langle n_p \rangle \ll \langle n_c \rangle$. On the other hand, in a VIT system, the control field is initially the vacuum, and the transparency window and group delay vary strongly with n_p, which sets n_c as described earlier. To demonstrate the strong optical nonlinearity intrinsic to the VIT system, we directly vary the average cavity photon number $\langle n_c \rangle$ by exciting the cavity mode with a weak laser beam, and measure the probe transmission. With the cooperativity η replaced by a free parameter, we fit the measured spectra (see lower inset to Fig. 4 as an example) using Eq. 1 and taking into account the spatial
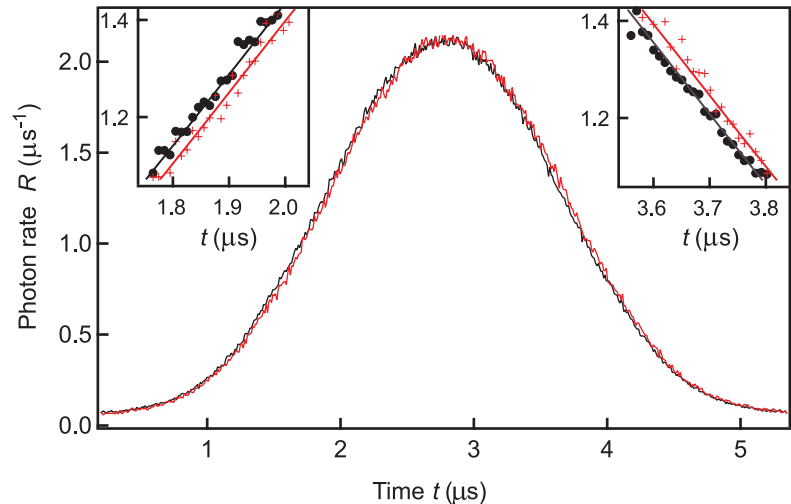
Fig. 3. Vacuum-induced group delay of a probe pulse. The black circles show the probe pulse in the absence of atoms; the red crosses indicate the probe pulse traveling through the atomic medium on VIT resonance $\Delta = \delta = 0$. The observed delay induced by the cavity vacuum field is $\tau = 25 \pm 2$ ns. The delayed pulse experiences absorption and has been rescaled by a factor of 1.6 for easier visualization of the group delay.

Fig. 4. VIT as a limiting case of EIT: Effective cooperativity $\tilde{\eta}$ at an antinode as a function of average cavity photon number $\langle n_c \rangle$ extracted from fits to measured spectra as shown in the lower right inset for $\langle n_c \rangle = 22$. The effective cooperativity is expected to scale as $\tilde{\eta} = \tilde{\eta}_0(\langle n_c \rangle + 1)$, and we find good agreement with a linear fit. The upper left inset shows the peak transparency Θ versus $\langle n_c \rangle$, demonstrating that even one control photon substantially changes the transmission. Error bars indicate $\pm 1\sigma$ standard deviation.
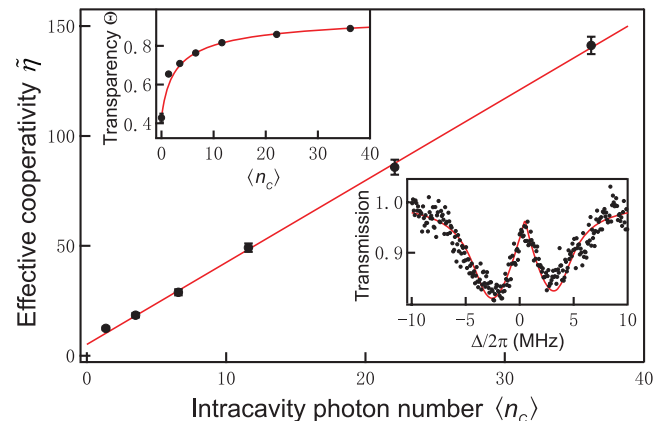
variation of the cavity coupling. Figure 4 shows the effective cooperativity thus extracted at an antinode $\tilde{\eta}$ versus $\langle n_c \rangle$. Because the control Rabi frequency is given by $\Omega_c = 2g\sqrt{n_c + 1}$, we expect a linear dependence of $\tilde{\eta}$ on $\langle n_c \rangle$ with a slope m equal to the y-axis intercept $\tilde{\eta}_0$. A linear fit to the data for $\langle n_c \rangle > 2$, where the atom-induced cavity line broadening has negligible effect, yields $m = 3.7 \pm 0.1$, $\tilde{\eta}_0 = 5 \pm 1$, and the ratio $\tilde{\eta}_0/m = 1.4 \pm 0.3$, in reasonable agreement with the model that predicts $m = \tilde{\eta}_0 = f_{eg}\eta_0 = 3.4$. The upper inset shows the peak transparency Θ versus $\langle n_c \rangle$. The transparency is defined as $\Theta = (T' - T)/(1 - T)$, where T' (T) denotes the resonant transmission with (without) the control field, and $T = \exp(-\mathcal{N}) = 0.67$. This plot shows that a substantial transparency increase over the vacuum-control level already occurs for one intracavity photon. In the future, it should be possible to use this effect in such applications as nondestructive measurement of the intracavity photon number (20, 21).

We have demonstrated that a vacuum field can generate a transparency window in an ensemble of three-level atoms and observed the associated group delay. By using a cavity-enhanced control field, we could substantially modify the transmission of an atomic ensemble with ~10

control photons. We also note that two probe beams, even when passing through spatially separated regions of the atomic ensemble, should influence each other's group velocity through the common interaction with the cavity mode, paving the way to cavity-mediated strong photon-photon interaction and quantum gates (1, 2). In such a geometry, the technical roadblocks associated with both cavity-coupling losses (2, 6, 7, 9) and motional and state control of single atoms (8, 29) are bypassed. More generally, this work offers the prospect of strongly nonlinear, multimode quantum optics, with a realistic outlook for advanced quantum devices operating coherently with single photons.

References and Notes

1. T. Pellizzari, S. A. Gardiner, J. I. Cirac, P. Zoller, *Phys. Rev. Lett.* **75**, 3788 (1995).
2. Q. A. Turchette, C. J. Hood, W. Lange, H. Mabuchi, H. J. Kimble, *Phys. Rev. Lett.* **75**, 4710 (1995).
3. A. Rauschenbeutel et al., *Phys. Rev. Lett.* **83**, 5166 (1999).
4. D. Chang et al., *Nat. Phys.* **4**, 884 (2008).
5. G. Rempe, R. J. Thompson, R. J. Brecha, W. D. Lee, H. J. Kimble, *Phys. Rev. Lett.* **67**, 1727 (1991).
6. R. J. Thompson, G. Rempe, H. J. Kimble, *Phys. Rev. Lett.* **68**, 1132 (1992).
7. P. Münstermann, T. Fischer, P. Maunz, P. W. H. Pinkse, G. Rempe, *Phys. Rev. Lett.* **82**, 3791 (1999).
8. K. M. Birnbaum et al., *Nature* **436**, 87 (2005).
9. I. Fushman et al., *Science* **320**, 769 (2008).
10. S. E. Harris, *Phys. Rev. Lett.* **62**, 1033 (1989).
11. S. Harris, Y. Yamamoto, *Phys. Rev. Lett.* **81**, 3611 (1998).
12. M. Fleischhauer, A. Imamoglu, J. Marangos, *Rev. Mod. Phys.* **77**, 633 (2005).
13. K.-J. Boller, A. Imamolu, S. E. Harris, *Phys. Rev. Lett.* **66**, 2593 (1991).
14. M. M. Kash et al., *Phys. Rev. Lett.* **82**, 5229 (1999).
15. L. V. Hau, S. E. Harris, Z. Dutton, C. H. Behroozi, *Nature* **397**, 594 (1999).
16. M. Bajcsy et al., *Phys. Rev. Lett.* **102**, 203902 (2009).
17. J. E. Field, *Phys. Rev. A* **47**, 5064 (1993).
18. P. R. Rice, R. J. Brecha, *Opt. Commun.* **126**, 230 (1996).
19. G. Nikoghosyan, M. Fleischhauer, *Phys. Rev. Lett.* **105**, 013601 (2010).
20. C. Guerlin et al., *Nature* **448**, 889 (2007).
21. D. I. Schuster et al., *Nature* **445**, 515 (2007).
22. M. Mücke et al., *Nature* **465**, 755 (2010).
23. T. Kampschulte et al., *Phys. Rev. Lett.* **105**, 153603 (2010).
24. H. Tanji-Suzuki et al., arxiv:quant-ph/1104.3594 (2011).
25. S. Gupta, K. L. Moore, K. W. Murch, D. M. Stamper-Kurn, *Phys. Rev. Lett.* **99**, 213601 (2007).
26. F. Brennecke et al., *Nature* **450**, 268 (2007).
27. Y. Colombe et al., *Nature* **450**, 272 (2007).
28. V. Vuletić, C. Chin, A. J. Kerman, S. Chu, *Phys. Rev. Lett.* **81**, 5768 (1998).
29. S. Nußmann et al., *Phys. Rev. Lett.* **95**, 173602 (2005).

Single-Shot Correlations and Two-Qubit Gate of Solid-State Spins

K. C. Nowack,[1]* M. Shafiei,[1] M. Laforest,[1]† G. E. D. K. Prawiroatmodjo,[1] L. R. Schreiber,[1] C. Reichl,[2] W. Wegscheider,[2] L. M. K. Vandersypen[1]*

Measurement of coupled quantum systems plays a central role in quantum information processing. We have realized independent single-shot read-out of two electron spins in a double quantum dot. The read-out method is all-electrical, cross-talk between the two measurements is negligible, and read-out fidelities are ~86% on average. This allows us to directly probe the anticorrelations between two spins prepared in a singlet state and to demonstrate the operation of the two-qubit exchange gate on a complete set of basis states. The results provide a possible route to the realization and efficient characterization of multiqubit quantum circuits based on single quantum dot spins.

For the efficient implementation and characterization of quantum information protocols, the ability to measure multiple qubits individually and in a single-shot manner is crucial (1, 2). The key reason is that output states are often entangled quantum superpositions. If only one qubit is read out after every protocol run, the protocol must be repeated to measure successive bits, the superposition may collapse to a different state after every run, and correlations between the

bits will possibly be lost. Joint measurements that require averaging over many runs pose similar problems, as various collapses contribute to the result. In contrast, independent single-shot measurement of all qubits gives full information from one collapse, which means that information contained in the (quantum) correlations can be obtained in the measurement.

A promising platform for realizing quantum protocols is provided by spins in the solid state, as they are well-isolated from the environment yet can be well controlled (3, 4). Spin detection has been pushed to the single-spin level with the use of magnetic resonance force microscopy (5), scanning tunneling microscopy (6, 7), optical spectroscopy (8–10), and transport spectroscopy (11–13).

Single-shot read-out of individual spins requires accumulation of a signal sufficiently strong

to distinguish two spin states before the spin decays. Electrical single-shot read-out of a single electron spin has been realized in gate-defined quantum dots (14, 15) and for a P impurity in Si (16). Optical single-shot read-out was achieved for a nuclear spin next to a diamond nitrogen-vacancy center (17) and for an electron spin in a self-assembled quantum dot (18). On two-electron systems, electrical single-shot read-out has been demonstrated as well (19, 20), but only one bit of information was obtained on the joint state of the two spins.

Extending existing methods to independent read-out of two spins is not trivial: (i) Measurement of the first spin must be sufficiently noninvasive to allow subsequent measurement of the other. (ii) Independent read-out requires a vanishing coupling between the two spins, whereas a finite coupling is required for universal control of the spins. (iii) While the first spin is being measured, the second spin is subject to relaxation, which places tight restrictions on the read-out duration, hence the signal-to-noise ratio.

Here we demonstrate independent single-shot read-out of two electron spins in a double quantum dot, show that there is negligible cross-talk between the two measurements, and probe the correlations between the respective measurement outcomes for a variety of input states. The read-out allows us to demonstrate and benchmark the operation of the two-qubit exchange gate on a complete set of input states.

Our double quantum dot is formed by using Ti/Au surface gates to locally deplete a two-

[1]Kavli Institute of Nanoscience, Delft University of Technology, Post Office Box 5046, 2600 GA Delft, Netherlands. [2]Solid State Physics Laboratory, ETH Zurich, Schafmattstrasse 16, 8093 Zurich, Switzerland.

*To whom correspondence should be addressed. E-mail: k.c.nowack@tudelft.nl (K.C.N.), l.m.k.vandersypen@tudelft.nl (L.M.K.V.)
†Present address: Institute for Quantum Computing, University of Waterloo, Waterloo, Ontario, N2L 3G1 Canada.

Vacuum-Induced Transparency
Haruka Tanji-Suzuki, Wenlan Chen, Renate Landig, Jonathan
Simon and Vladan Vuletic (August 4, 2011)
Science **333** (6047), 1266-1269. [doi: 10.1126/science.1208066]
originally published online August 4, 2011

Editor's Summary

Article Tools	Visit the online version of this article to access the personalization and article tools: http://science.sciencemag.org/content/333/6047/1266
Permissions	Obtain information about reproducing this article: http://www.sciencemag.org/about/permissions.dtl